Inorganic Chemistry

pubs.acs.org/IC Article

Distribution of Spin Density on Phenoxyl Radicals Affects the Selectivity of Aerobic Oxygenation of Phenols

Yongtao Wang,[‖] Jun Guan,[‖] Bingbao Mei, Mengtian Fan, Rui Lu, Renfeng Du, Kaizhou Chen, Jia Yao, Zheng Jiang,* and Haoran Li*

Cite This: https://dx.doi.org/10.1021/acs.inorgchem.9b02422 Read Online

ACCESS | Metrics & More | Article Recommendations | Supporting Information

ABSTRACT: Phenoxyl radical was generally suggested as the intermediate during copper-catalyzed aerobic oxygenation of phenols. However, the substrate-dependent selectivity has not been well interpreted, due to insufficient characterization of the radical intermediate under reaction conditions. When studying the CuCl-LiCl-catalyzed aerobic phenol oxidation, we obtained EPR spectra of phenoxyl radicals generated by oxidizing phenols with the preactivated catalyst. Upon correlation to the selectivity of benzoquinone, the hyperfine coupling constant of *para*-site proton ($a^{H,\,para}$) was found to be better than the Hammett constant. The catalysis mechanism was studied based on EPR detection and the reaction results of phenoxyl radicals under N_2 or O_2 atmosphere. It appeared that the chemoselectivity depended on the attack of activated dioxygen on phenoxyl radicals, and the activation of dioxygen by $[Cu_nCl_{n+1}]^-$ (n = 1, 2, 3) was suggested as the rate-determining step. Understanding of the substrate-dependent selectivity contributed to predicting the chemoselectivity in the aerobic oxidation of phenols.

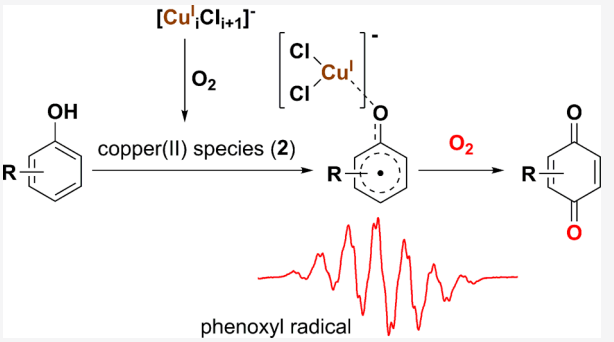

INTRODUCTION

The copper-catalyzed aerobic oxidation of phenols is not only a crucial process in the body but also of great importance in industrial processes.[1] During the industrial production of vitamin E, the oxidation of 2,3,6-trimethylphenol (2,3,6-TMP) to 2,3,5-trimethyl-1,4-benzoquinone (TMBQ) is a crucial process,[2] where the most-used catalyst is $CuCl_2$ with additives (such as LiCl, $NH_2OH{\cdot}HCl$, and ionic liquids).[3] For various *para*-hydrogen-substituted phenols, great efforts have been made to control the oxygenation selectivity,[1a,4] and a pathway via phenoxyl radical is recommended.[5] Our recently reported work concerned the $CuCl_2$-catalyzed aerobic oxidation of 2,3,6-TMP[5b] and suggested that the TMBQ was majorly formed by the attack of activated O_2 on the phenoxyl radicals. As a side reaction, polymerizations go through the same intermediate, and the radical intermediate was suggested to exist as a copper(I)−phenoxyl radical, which has a resonance structure as copper(II)−phenolate.[6]

The substrate-dependent selectivity of oxygenation is significant.[1a] For instance, 2,6-di-*tert*-butylphenol (2,6-DTBP) is much easier to produce benzoquinones than 2,6-dimethylphenol, which is easier to polymerize.[7] Moreover, for the cross-coupling of phenols, the regioselectivity was also found to be substrate dependent,[8] and a pathway through phenoxyl radicals was recommended. Commonly, Hammett constants were used to evaluate the reactivity of different substrates; however, the reactivity at *para* carbon may be not very relevant to the Hammett constant, which is more suitable for the reactivity at hydroxyl oxygen. Therefore, the more suitable factor needs to be developed for phenol oxygenation.

There should be a relationship between the nature of the phenoxyl radical and the oxygenation selectivity. However, a clear description of this relationship is still absent, because only sterically stabilized phenoxyl radicals, like 2,6-di-*tert*-butylphenoxyl radicals, are well characterized.[9] Müller et al. have isolated the 2,6-di-*tert*-butyl-4-Ph-phenoxyl radical,[10] and Mayer and co-workers have isolated and well characterized the 2,4,6-tri-*tert*-butylphenoxyl radical and 2,6-di-*tert*-butyl-4-(4′-nitrophenyl)phenoxyl radical.[11] Furthermore, with electron paramagnetic resonance (EPR), Brigati et al. have investigated many *para*-substituted 2,6-di-*tert*-butyllphenoxyl radicals and revealed the relationship between the hyperfine coupling constant of *meta* protons and the O−H bond dissociation enthalpy.[12]

Recently, we reported a solvent effect study on the copper-catalyzed oxidation of 2,3,6-TMP,[13] in which the active state of catalyst was simulated by the reaction between CuCl−LiCl and dioxygen in alcohols. This species showed highly efficient

Received: August 10, 2019

https://dx.doi.org/10.1021/acs.inorgchem.9b02422
Inorg. Chem. XXXX, XXX, XXX−XXX

dehydrogenating activity on 2,3,6-TMP, giving the phenoxyl radical. By the same way in this work, we used the CuCl−LiCl catalyst as the model system and studied the aerobic oxidation of various *para*-hydrogen substituted phenols in *n*-hexanol. Moreover, we prepared the activated catalyst (**2**) by oxidizing CuCl−LiCl catalyst with O_2 and obtained phenoxyl radicals by oxidizing phenols with **2**. EPR spectra were collected for obtained phenoxyl radicals. Accordingly, an almost linear relationship was established between the hyperfine coupling constant of the *para*-site proton and the yield of benzoquinone during the catalytic oxidation. Moreover, this relationship was interpreted via further mechanistic study.

RESULTS AND DISCUSSION

CuCl−LiCl Catalyzed Oxidation of *para*-Hydrogen-Substituted Phenols. The CuCl−LiCl catalyst system was used in this study, where LiCl was the cocatalyst to provide Cl^- and to help increase the solubility of CuCl. Suggested by ESI mass spectrum results, the CuCl−LiCl catalyst existed in *n*-hexanol as $[Cu_nCl_{n+1}]^-$ (n = 1, 2, 3) (**1**) (Figure S3). We explored the catalytic performance of the CuCl−LiCl system on the oxidation of 2,3,6-TMP (**4a**) and 2,6-di-*tert*-butylphenol 2,6-DTBP (**4b**) in *n*-hexanol. The main products were detected to be benzoquinones, the same as that in a $CuCl_2$-catalyzed system (Scheme 1). The side reaction was found to

Scheme 1. Catalytic Oxidation of 2,3,6-TMP and 2,6-DTBP

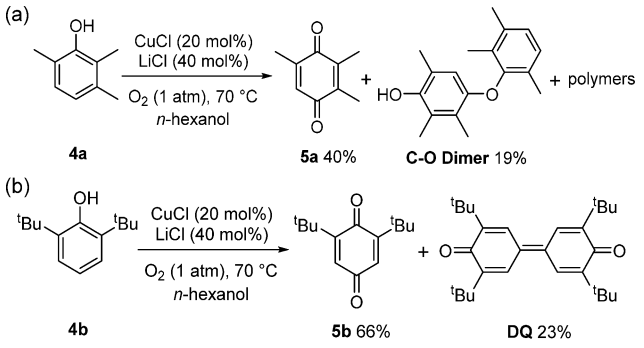

be dimerization and polymerization, leading to dimer, polymers (detected by GPC, Figure S1), or biphenylquinone (**DQ**). At full conversion, the yield of benzoquinone from 2,6-DTBP (66%) was higher than that from 2,3,6-TMP (40%).

Moreover, for 2-*tert*-butyl-6-methylphenol (**4c**), 2,3,5-trimethylphenol (**4d**), 2-methyl-5-*iso*-propylphenol (**4e**), 2,6-dimethylphenol (**4f**), 2-*iso*-propyl-5-methylphenol (**4g**), and 1-naphthol (**4h**), the yields of benzoquinones were also obtained at 100% conversion, as shown in Scheme 2.

Factors Causing the Different Yields of Benzoquinone. Suggested by Hay et al.,[7a] the high selectivity of **5b** was caused by the steric effect of ^{t}Bu- group at the *ortho* site of **4b**. However, with a less steric group at the *ortho* site, **4d**, **4g**, and **4h** gave more benzoquinone than **4a** and **4f**, and thus, the steric effect could not be the main factor influencing the selectivity. We tried to correlate the yield of benzoquinone with the total Hammett constant (σ) of substituted groups, which was obtained by adding the corresponding values of σ_m and σ_o.[14] As shown in Figure 1, the benzoquinone yield was poorly related with the total Hammett constant (R^2 = 0.008). These Hammett constants were determined by the ^{1}H NMR chemical shift of OH in substituted phenols; therefore, the

Scheme 2. Yields of 5 for CuCl−LiCl-Catalyzed Aerobic Oxidations

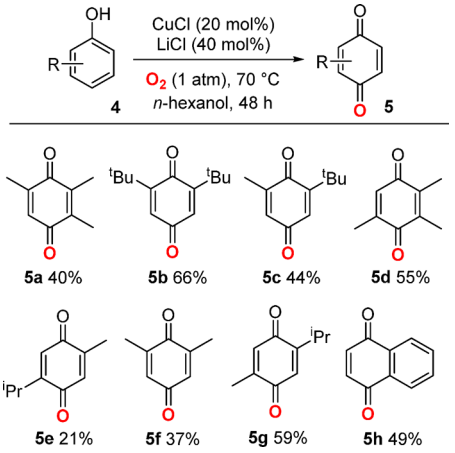

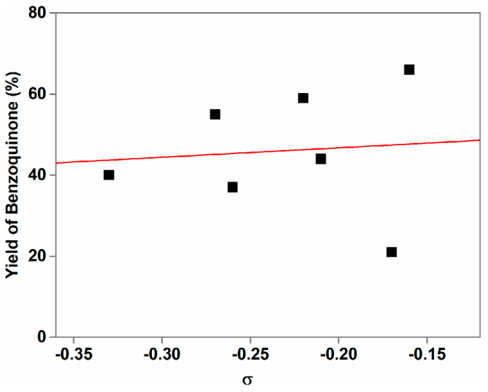

Figure 1. Relationship between the yield of benzoquinones and the total Hammett constant (σ). The data were fitted with the linear function (red line): $y = 23.3x + 51.4$, $R^2 = 0.008$.

selectivity should not depend on the electron distribution at the hydroxyl oxygen.

Measurement of *para*-Site Spin Density at Phenoxyl Radicals. The phenoxyl radical is the intermediate for both oxygenation and oxidative coupling, and its unpaired electron is delocalized and shared by the oxygen, *ortho*-carbon, and *para*-carbon. We anticipated that the distribution of spin density, which is affected by the substituent groups, may cause the different selectivities of benzoquinone for different phenols.

We began our investigations by oxidizing the phenols with activated copper species **2**, and we characterized the phenoxyl radicals corresponding to **4a**−**4h** with EPR. **2** was generated by the reaction between **1** and dioxygen, and the characterizations suggested it as an antiferromagnetically coupled copper(II) species. Further characterizations on **2** is discussed in the Supporting Information. After adding phenols into the solution of **2** at N_2 atmosphere, we immediately collected EPR spectra for the solution and observed radical signals (Figure 2, black). The copper(II) species, like (μ−η^2:η^2-peroxo)dicopper(II) complex, has also been reported to oxidize phenols toward phenoxyl radicals.[15]

Different from the copper(II)−phenolate isolated by Higashimura et al.,[6a−c] the phenoxyl radical we observed was rather a "free" radical, though it was reasonable to assume a copper(I) linked on it due to the broadened EPR signal. By performing EPR simulations using Easyspin,[16] the simulated

https://dx.doi.org/10.1021/acs.inorgchem.9b02422
Inorg. Chem. XXXX, XXX, XXX−XXX

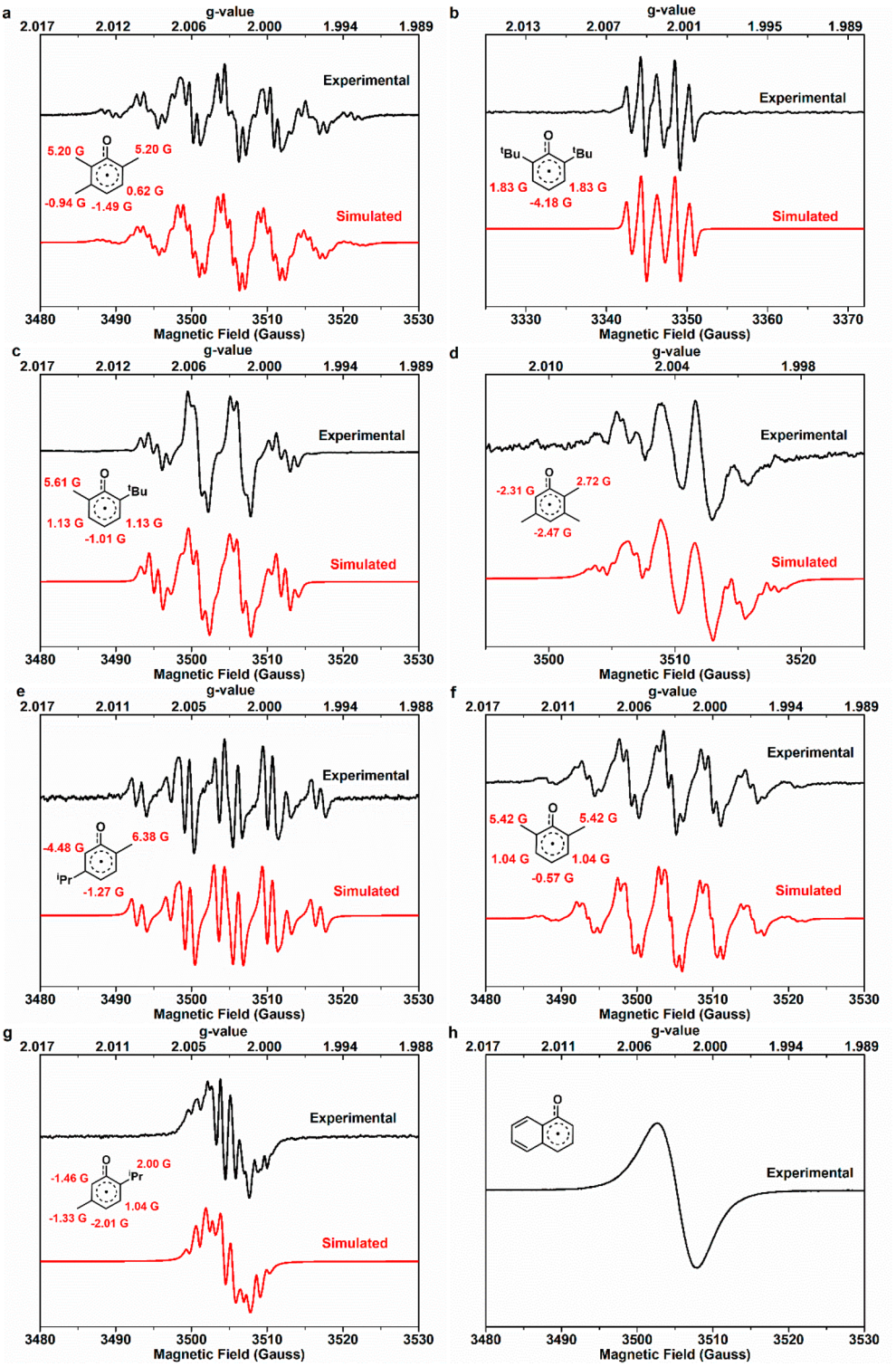

Figure 2. Experimental (black) and simulated (red) X-band EPR spectra of phenoxyl radicals corresponding to **4a** (a), **4b** (b), **4c** (c), **4d** (d), **4e** (e), **4f** (f), **4g** (g), and **4h** (h) and the simulated hyperfine coupling constants were given in gauss. The radicals were formed upon addition of phenols to a *n*-hexanol solution of **2** at room temperature.

values of isotropic hyperfine splitting of proton (a^H) were obtained for each radical, and we ignored the a^H lower than the half-peak width.

According to the splitting types and simulated a^H values, these signals were assigned to phenoxyl radicals corresponding to **4a**−**4g**, respectively (Figure 2). Moreover, DFT calculations were performed to help assign a^H for protons with the same splitting pattern (Figure S11). Though the calculation was not so good, it can be found that the coordination of phenoxyl radicals at copper(I) had apparent influence on the a^H, which could be the reason for different a^H from reported values in the literature.[17] Nevertheless, the coordination Gibbs free energy for 2,6-di-*tert*-butyl phenoxyl radical was 7.7 kcal/mol, and the energy was 2.0 kcal/mol for the 2,6-dimethyl phenoxyl radical.

https://dx.doi.org/10.1021/acs.inorgchem.9b02422
Inorg. Chem. XXXX, XXX, XXX−XXX

Therefore, the coordination for the 2,6-dimethyl phenoxyl radical on copper(I) was much easier than that for 2,6-di-*tert*-butyl phenoxyl radical. Thus, it should be reasonable that the *para* a^H we obtained for the 2,6-dimethyl phenoxyl radical was much smaller than that of the 2,6-di-*tert*-butyl phenoxyl radical. Moreover, the EPR spectrum from **4h** just showed a broad peak, which should be caused by too many protons with close but different a^H values; thus, the a^H values could not be obtained.

Arising from the magnetic interaction between an unpaired electron and a proton, a^H provides important information about the distribution of spin density. McConnell's relationship points that a^H reveals the spin density (ρ) on the adjacent carbon atom ($a^H = -Q\rho$, where Q is a constant for the similar system).[18] As a result of the resonance stabilization, other than the hydroxyl oxygen, the spin density distributes mainly on the *ortho*- and *para*-site of phenoxyl radicals.

Therefore, the phenoxyl radical from **4f** possessed the least spin density at the *para*-carbon, while the phenoxyl radical from **4b** possessed the most. Moreover, it could be found that 2,6-di-*tert*-butyl-substituted radicals had more spin density at the *para*-site than 2,6-dimethyl substituted radicals. Using the same method, the phenoxyl radicals from 2,4,6-trimethylphenol as well as 2,6-di-*tert*-bultyl-4-methylphenol were also observed (Figure S12), and the a^H at the *para*-methyl group of 2,4,6-trimethylphenol (1.03 gauss) was much less than that of 2,6-di-*tert*-bultyl-4-methylphenol (11.2 gauss).

Correlation of $a^{H,\,para}$ and the Yield of Benzoquinone. A linear correlation was suggested between the yield of benzoquinones and the hyperfine coupling constant of the *para*-site proton, $a^{H,\,para}$ (Figure 3, $R^2 = 0.586$). Consequently,

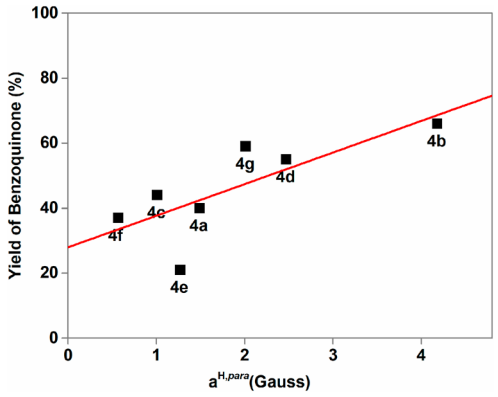

Figure 3. Relationship between the yield of benzoquinones **5a**–**5d**, **5f**, and the hyperfine coupling constant of *para*-site proton ($a^{H,\,para}$) at the phenoxyl radical. The data were fitted with the linear function (red line): $y = 9.73x + 27.9$, $R^2 = 0.586$.

the distribution of spin density could be a crucial factor for the selectivity between oxidative coupling and oxygenation. More spin density at the *para*-carbon should lead to increasing selectivity of benzoquinone. The interpretation for this relationship will be discussed later, after the mechanism investigations.

Origin of the Relationship. The relationship between quinone selectivity and $a^{H,\,para}$ may be interpreted by the reactivity of the phenoxyl radical. The GC-FID and GC-MS analyses were carried out to detect what was produced from these phenoxyl radicals. As shown in Scheme 3, no benzoquinone was formed when 2,3,6-TMP (**4a**) and 2,6-

Scheme 3. Reaction Results between 2 and Phenols

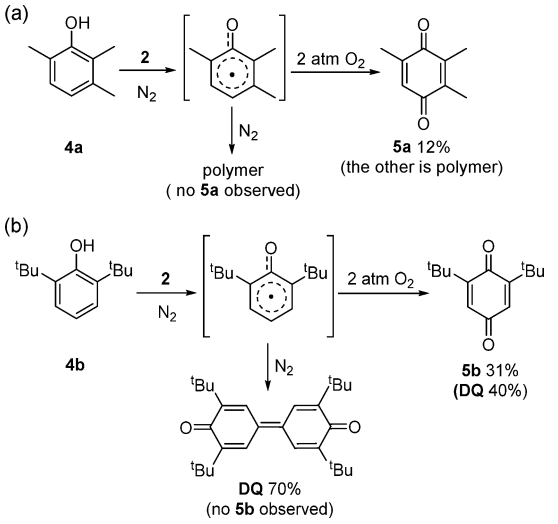

DTBP (**4b**) reacted with excess **2** under N_2 atmosphere. However, when the reaction was performed under 2 atm O_2, 12% and 31% benzoquinone was obtained from **4a** and **4b**, respectively. The main byproduct was the polymers for 2,3,6-TMP (according to GPC analysis, Figure S13) and biphenylquinone (**DQ**) for *p*-H-DTBP (70% under N_2, 40% under O_2). Moreover, the $^{18}O_2$-labling experiment was performed to confirm the oxygen source. When **4a** reacted with excess **2** under 2 atm $^{18}O_2$ atmosphere, the GC-MS analyses revealed that ^{18}O was incorporated into **5a** with a proportion of ~70% (Figure S14). This result is consistent with the catalytic oxidation result, where **5a** was proposed to be partially generated from the C–C dimer, and the oxygen of **5a** should come from water.[3c]

Consequently, under N_2 atmosphere, phenoxyl radicals could only polymerize and give rise to polymers. Under O_2 atmosphere, however, phenoxyl radicals could react with O_2 to form benzoquinones. Based on the work of Berho and Lesclaux,[19] no reaction was observed between phenoxyl radical and O_2, thus O_2 must be activated. By DFT investigations, Ghosh et al. recommended a bridging copper(II)–peroxoquinone complex as the intermediate to form benzoquinones.[20] Further, the superoxo–cobalt(III) complex,[21] superoxo–nickel(II) complex,[22] and superoxo–copper(II) complex[5a] were suggested to attack the phenoxyl radicals to form benzoquinones. Consequently, the formation of quinones was supposed here via the attack of cooper(I)-activated O_2 (the superoxo–copper(II) complex (**3**)) on the phenoxyl radicals.

The reaction of phenoxyl radical with activated dioxygen (**3**) controlled the chemoselectivity. The attack of **3** on phenoxyl radical was a reaction between two radicals, i.e., between the p orbital of *para*-site carbon and p orbital of oxygen (Figure 4).

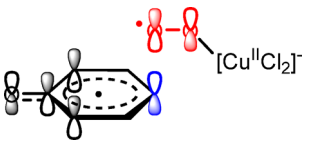

Figure 4. Diagram of SOMO orbitals for a phenoxyl radical and activated dioxygen (**3**).

https://dx.doi.org/10.1021/acs.inorgchem.9b02422
Inorg. Chem. XXXX, XXX, XXX–XXX

As discussed before, the larger a^H of *para*-site proton indicates the greater spin density at *para*-site carbon, which means a higher SOMO coefficient for the p orbital of *para*-carbon. Additionally, the coefficients of the frontier molecular orbital have been successfully used to evaluate the regioselectivity and reactivity of addition reactions.[23] A higher SOMO coefficient for the p orbital of *para*-carbon should lead to higher selectivity and higher reactivity for the formation of benzoquinone. Consequently, it could be reasonable that the regioselectivity was positively correlated with the a^H of *para*-site proton at the phenoxyl radical.

Proposed Mechanism. During the process of CuCl−LiCl-catalyzed oxidation of 2,3,6-TMP (Scheme 1a), the same phenoxyl radical as that obtained by the reaction between **2** and 2,3,6-TMP was suggested by EPR. Consequently, the resting state of the catalyst should be a copper(I) species (**1**), along with the phenoxyl radical (Figure 5).

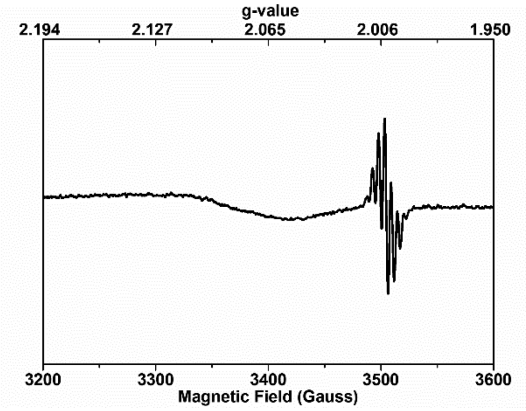

Figure 5. X-band EPR spectrum detected at 5 h of the catalysis reaction shown in Scheme 1a.

The proposed catalysis mechanism is shown in Scheme 4. The reaction was initialized by the reaction between dioxygen

Scheme 4. Proposed Mechanism

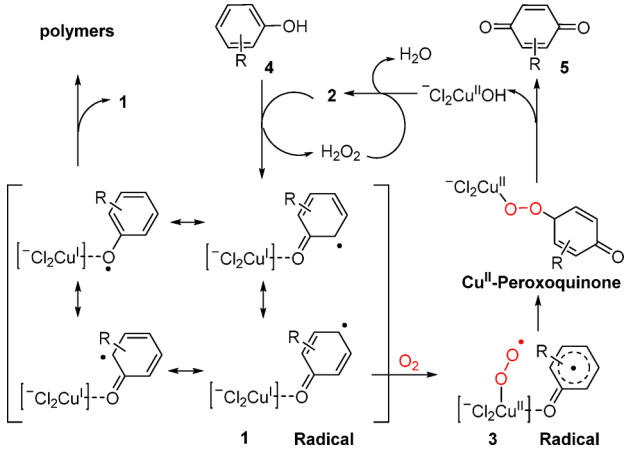

and the catalyst **1**, giving the activated catalyst **2**. **2** oxidized phenols with its effective dehydrogenating activity, yielding phenoxyl radicals and **1**, as well as H_2O_2. The activating of dioxygen by **1** was recommended as the rate-determining step and led to the formation of **3**. For phenoxyl radical with more spin density at the *para*-site, its reaction with **3** should be preferred, resulting in a higher yield of benzoquinone. However, for phenoxyl radicals with more spin density at the hydroxyl oxygen, the C−O polymerization among radicals should be preferred, leading to decreasing the yield of benzoquinone. The C−O dimer was included in the polymers in Scheme 4.

The production of benzoquinones was suggested here to go through a bridging copper(II)−peroxoquinone complex, and the $[Cl_2Cu^{II}OH]^-$ was generated along with the product. Kitajima et al. have prepared the ^{S}**P** type Cu/O_2 species by the reaction of LCu(II)OH complex with H_2O_2;[24] thus, we proposed that **2** was generated by reaction between $[Cl_2Cu^{II}OH]^-$ and H_2O_2. The $[Cl_2Cu^{II}OH]^-$ was suggested to be a bis(μ-hydroxo)dicopper(II,II) species (Figure S9B, Table S2) and was nearly EPR silent (Figure S15, black). Its reaction with 2,3,6-trimethylphenol only showed the mononuclear Cu(II) signal in the EPR spectrum (Figure S15, red), while the reaction of **2** with 2,3,6-trimethylphenol showed the phenoxyl radical signal and no mononuclear Cu(II) signal (Figure S15, purple). Thus, the $[Cl_2Cu^{II}OH]^-$ could not oxidize phenols to phenoxyl radicals.

To verify the proposed mechanism, we investigated the change of quinone concentration with reaction time. The formation of quinones at the beginning of the reaction could be well fitted with the linear function (Figure S16). Based on the proposed mechanism, the formation rate of quinones should also be affected by the distribution of spin density. Consequently, when correlating the fitted formation rate with $a^{H,\,para}$ at phenoxyl radical, we obtained a positive relationship (Figure 6), which corresponded to the proposed mechanism.

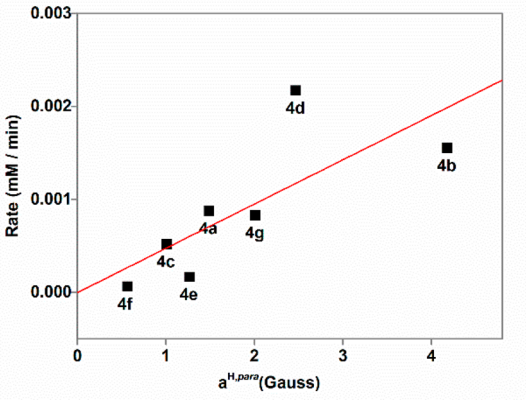

Figure 6. Relationship between the formation rate of benzoquinones **5a**−**5g** and the hyperfine coupling constant of *para*-site proton ($a^{H,\,para}$) at the phenoxyl radical. The data were fitted with the linear function (red line): $y = 0.000475x$, $R^2 = 0.573$.

CONCLUSION

In summary, the substrate-dependent benzoquinone selectivity was interpreted with the distribution of spin density at the phenoxyl radical. The positive linear relationship was established between the $a^{H,\,para}$ and the yield of benzoquinones. Phenoxyl radicals were detected after the oxidation of phenols with **2**, which was the simulated activated catalyst during the reaction, and was formed by the oxidation of the catalyst (**1**) with dioxygen. It was found that phenoxyl radicals could only polymerize under N_2 atmosphere but could produce benzoquinones under O_2 atmosphere. Consequently, while

https://dx.doi.org/10.1021/acs.inorgchem.9b02422
Inorg. Chem. XXXX, XXX, XXX−XXX

polymers were formed by the reaction among radicals, the main pathway to produce benzoquinones was proposed to be the attack of activated O_2 on phenoxyl radicals, and the phenoxyl radical with higher spin density at its *para*-carbon should prefer this pathway rather than the competitive coupling. These findings contribute to our understanding of the aerobic oxidation of phenols, as well as to the nature of phenoxyl radicals. We hope this work could provide a clue for the control of selectivity in phenol oxidations.

EXPERIMENTAL SECTION

General Methods. All reagents were purchased from commercial sources without further treatment unless otherwise noted. UV−vis experiments were carried out on a TU-1901 spectrophotometer (Purkinje General Instrument Co., Ltd., China) equipped with a thermostat using a 1 cm modified cuvette. UV−vis−NIR spectra were recorded on a UV-3600 Shimadzu spectrophotometer using a 1 cm cuvette. CV was performed on a CHI630 electrochemical analyzer (CH Instrument, China). The CW-EPR spectra were recorded on a Bruker A300 EPR spectrometer at 9.8 GHz. Electrospray ionization−mass spectrometry (ESI-MS) measurements were performed on an Agilent 1260/6120 mass spectrometer (Agilent, America), and the detection was in negative ion modes. Gas chromatography−mass spectrometry (GC-MS) experiments were carried out on a Shimadzu GC/MS-QP2010 system (Shimadzu, Germany). GC-FID measurements were performed on GC-2010 (Shimadzu, Japan) instrument. Gel permeation chromatography (GPC) was performed at Waters 2515 with an RI 2414 as the detector.

Catalytic oxidation of phenols. In a two-neck flask (25 mL) equipped with a magnetic stir bar, 5 mmol phenol, 1 mmol CuCl, and 2 mmol LiCl were added with 10 mL of *n*-hexanol. The mixture was stirred under N_2 atmosphere for dissolution, and then the N_2 was replaced by O_2 and an O_2 balloon (1 atm) was equipped. The reaction was performed at 343 K and 800 rpm. The commercial reactants and products were used as the standard for gas chromatography. The conversion and yield were determined by gas chromatography using the standard curve, and the products were detected by GC-MS and GPC.

Formation of the activated catalyst 2. In the glovebox, a 0.09 M solution of complex **1** was prepared by adding 1.5 mmol of CuCl and 3 mmol of LiCl to 15 mL of *n*-hexanol, and the mixture was stirred at 333 K for 3 h. After filtration, the filtrate was characterized by spectroscopy. The concentration of copper ion in the filtrate was measured to be 0.0887 M using atomic absorption spectroscopy (AAS). In the glovebox, 6.2 mL of 0.09 M *n*-hexanol solution of **1** (the filtrate) was injected into a pressure-resistant reaction flask. After it was removed from the glovebox, the flask was charged with 1 atm O_2, and another 20.0 mL of O_2 was injected in via a gastight syringe; then, the solution was stirred at room temperature for 5 h. The reacted O_2 was quantified by a gastight syringe to be 5.5 mL. The concentration of Cu(II) was calculated to be 82 mM (92% of total copper) by comparing the d−d transition bands with standard $CuCl_2$ solution in *n*-hexanol. Thus, a Cu^{II}/O_2 ratio of 2.07:1 was obtained for **2**. The dark brown species **2** persists for several days at room temperature but precipitates immediately with small amount of water or methanol.

EPR Spectroscopy. To detect phenol radicals, the fully generated solution of **2** was packed in a 5 mm quartz EPR sample tube sealed with a rubber cap. After purging with N_2, the radical was formed by the addition of a stock solution of phenols and was immediately detected at 298 K. The least-squares fittings of EPR spectra were performed using Easyspin 5.1[16] with the garlic function.

Oxidation of Phenols by 2. The *n*-hexanol solution of **2** was prepared by stirring the *n*-hexanol solution of **1** under 2 atm O_2 at room temperature for 5 h, and then the solution was purged by three N_2/vacuum purge cycles. Next, 1.5 mL of solution of **2** was injected into a pressure-resistant reaction flask charged with 1 atm N_2 or 2 atm O_2. The concentrated *n*-hexanol solution of phenols (0.02 mmol) was injected into the flask at room temperature to start the reaction. The excess **2** was used here for full conversion. After 10 min, the reaction was quenched by 0.5 mL of water; the yields were determined by gas chromatography, and the products were detected by GC-MS and GPC.

ASSOCIATED CONTENT

Supporting Information

The Supporting Information is available free of charge at https://pubs.acs.org/doi/10.1021/acs.inorgchem.9b02422.

Additional experimental details and spectral data (PDF)

AUTHOR INFORMATION

Corresponding Authors

Zheng Jiang − *Shanghai Synchrotron Radiation Facility, Shanghai Institute of Applied Physics, Chinese Academy of Sciences, Shanghai 201204, P. R. China;* orcid.org/0000-0002-0132-0319; Email: jiangzheng@sinap.ac.cn

Haoran Li − *Department of Chemistry, ZJU-NHU United R&D Center and State Key Laboratory of Chemical Engineering, College of Chemical and Biological Engineering, Zhejiang University, Hangzhou 310027, P. R. China;* orcid.org/0000-0001-5294-8731; Email: lihr@zju.edu.cn

Authors

Yongtao Wang − *Department of Chemistry, ZJU-NHU United R&D Center, Zhejiang University, Hangzhou 310027, P. R. China*

Jun Guan − *Department of Chemistry, ZJU-NHU United R&D Center, Zhejiang University, Hangzhou 310027, P. R. China*

Bingbao Mei − *Shanghai Synchrotron Radiation Facility, Shanghai Institute of Applied Physics, Chinese Academy of Sciences, Shanghai 201204, P. R. China*

Mengtian Fan − *Department of Chemistry, ZJU-NHU United R&D Center, Zhejiang University, Hangzhou 310027, P. R. China*

Rui Lu − *Department of Chemistry, ZJU-NHU United R&D Center, Zhejiang University, Hangzhou 310027, P. R. China;* orcid.org/0000-0001-8734-097X

Renfeng Du − *Department of Chemistry, ZJU-NHU United R&D Center, Zhejiang University, Hangzhou 310027, P. R. China*

Kaizhou Chen − *Department of Chemistry, ZJU-NHU United R&D Center, Zhejiang University, Hangzhou 310027, P. R. China*

Jia Yao − *Department of Chemistry, ZJU-NHU United R&D Center, Zhejiang University, Hangzhou 310027, P. R. China;* orcid.org/0000-0002-7147-5973

Complete contact information is available at: https://pubs.acs.org/10.1021/acs.inorgchem.9b02422

Author Contributions

‖These authors contributed equally.

Funding

This work was supported by the National Natural Science Foundation of China (21573196), the Fundamental Research Funds of the Central Universities, and the National High Technology Research and Development Program (863 Program) of China (SS2015AA020601).

Notes

The authors declare no competing financial interest.

■ ACKNOWLEDGMENTS

The authors would like to gratefully thank Hongxian Han and Zhaochi Feng from the Dalian Institute of Chemical Physics, Chinese Academy of Sciences, and Jiadan Xue from the Department of Chemistry, Zhejiang Sci-Tech University, for resonance Raman spectroscopy. The authors also thank Xinyu Wang and Fahe Cao from the Department of Chemistry, Zhejiang University, for EPR and cyclic voltammograms.

■ REFERENCES

(1) (a) Allen, S. E.; Walvoord, R. R.; Padilla-Salinas, R.; Kozlowski, M. C. Aerobic Copper-Catalyzed Organic Reactions. *Chem. Rev.* **2013**, *113*, 6234−6458. (b) Wendlandt, A. E.; Suess, A. M.; Stahl, S. S. Copper-Catalyzed Aerobic Oxidative C-H Functionalizations: Trends and Mechanistic Insights. *Angew. Chem., Int. Ed.* **2011**, *50*, 11062−87. (c) Punniyamurthy, T.; Rout, L. Recent Advances in Copper-Catalyzed Oxidation of Organic Compounds. *Coord. Chem. Rev.* **2008**, *252*, 134−154. (d) van der Vlugt, J. I.; Meyer, F. Homogeneous Copper-Catalyzed Oxidations. *Top. Organomet. Chem.* **2007**, *22*, 191−240.

(2) Bonrath, W.; Eggersdorfer, M.; Netscher, T. Catalysis in the Industrial Preparation of Vitamins and Nutraceuticals. *Catal. Today* **2007**, *121*, 45−57.

(3) (a) Takehira, K.; Shimizu, M.; Watanabe, Y.; Orita, H.; Hayakawa, T. A Novel Synthesis of Trimethyl-p-Benzoquinone: Copper (II)−Hydroxylamine Catalysed Oxygenation of 2,3,6-Trimethylphenol with Dioxygen. *J. Chem. Soc., Chem. Commun.* **1989**, 1705−1706. (b) Shimizu, M.; Watanabe, Y.; Orita, H.; Hayakawa, T.; Takehira, K. Synthesis of Alkyl Substituted p-Benzoquinones from the Corresponding Phenols Using Molecular Oxygen Catalyzed by Copper(II) Chloride-Amine Hydrochloride Systems. *Bull. Chem. Soc. Jpn.* **1992**, *65*, 1522−1526. (c) Bodnar, Z.; Mallat, T.; Baiker, A. Oxidation of 2,3,6-Trimethylphenol to Trimethyl-1,4-Benzoquinone with Catalytic Amount of $CuCl_2$. *J. Mol. Catal. A: Chem.* **1996**, *110*, 55−63. (d) Sun, H.; Harms, K.; Sundermeyer, J. Aerobic Oxidation of 2,3,6-Trimethylphenol to Trimethyl-1, 4-Benzoquinone with Copper (II) Chloride as Catalyst in Ionic Liquid and Structure of the Active Species. *J. Am. Chem. Soc.* **2004**, *126*, 9550−9551. (e) Wang, C.; Guan, W.; Xie, P.; Yun, X.; Li, H.; Hu, X.; Wang, Y. Effects of Ionic Liquids on the Oxidation of 2,3,6-Trimethylphenol to Trimethyl-1,4-Benzoquinone under Atmospheric Oxygen. *Catal. Commun.* **2009**, *10*, 725−727.

(4) (a) Ling, K.-Q.; Lee, Y.; Macikenas, D.; Protasiewicz, J. D.; Sayre, L. M. Copper(II)-Mediated Autoxidation of *tert*-Butylresorcinols. *J. Org. Chem.* **2003**, *68*, 1358−1366. (b) Evtushok, V. Y.; Suboch, A. N.; Podyacheva, O. Y.; Stonkus, O. A.; Zaikovskii, V. I.; Chesalov, Y. A.; Kibis, L. S.; Kholdeeva, O. A. Highly Efficient Catalysts Based on Divanadium-Substituted Polyoxometalate and N-Doped Carbon Nanotubes for Selective Oxidation of Alkylphenols. *ACS Catal.* **2018**, *8*, 1297−1307. (c) Wanna, W. H.; Ramu, R.; Janmanchi, D.; Tsai, Y.-F.; Thiyagarajan, N.; Yu, S. S. F. An Efficient and Recyclable Copper Nano-Catalyst for the Selective Oxidation of Benzene to p-Benzoquinone (p-BQ) Using H_2O_2(aq) in CH_3CN. *J. Catal.* **2019**, *370*, 332−346.

(5) (a) Lee, J. Y.; Peterson, R. L.; Ohkubo, K.; Garcia-Bosch, I.; Himes, R. A.; Woertink, J.; Moore, C. D.; Solomon, E. I.; Fukuzumi, S.; Karlin, K. D. Mechanistic Insights into the Oxidation of Substituted Phenols via Hydrogen Atom Abstraction by a Cupric-Superoxo Complex. *J. Am. Chem. Soc.* **2014**, *136*, 9925−9937. (b) Wang, G.; Wang, Y.; Yao, J.; Li, H. Insight into 2,3,6-Trimethylphenol Oxidation by Comparing the Difference between Cupric Acetate and Cupric Chloride Catalysis. *Mol. Catal.* **2019**, *472*, 10−16.

(6) (a) Higashimura, H.; Fujisawa, K.; Moro-oka, Y.; Kubota, M.; Shiga, A.; Terahara, A.; Uyama, H.; Kobayashi, S. Highly Regioselective Oxidative Polymerization of 4-Phenoxyphenol to Poly(1,4-Phenylene Oxide) Catalyzed by Tyrosinase Model Complexes. *J. Am. Chem. Soc.* **1998**, *120*, 8529−8530. (b) Fujisawa, K.; Iwata, Y.; Kitajima, N.; Higashimura, H.; Kubota, M.; Miyashita, Y.; Yamada, Y.; Okamoto, K.-i.; Moro-oka, Y. Synthesis, Structure and Reactivity of Phenoxo Copper(II) Complexes, Cu(OAr)(HB(3,5-Pr^i_2pz)$_3$) (Ar = C_6H_4-4-F, 2,6-$Me_2C_6H_3$, 2,6-$Bu^t_2C_6H_3$). *Chem. Lett.* **1999**, *28*, 739−740. (c) Higashimura, H.; Kubota, M.; Shiga, A.; Fujisawa, K.; Moro-oka, Y.; Uyama, H.; Kobayashi, S. Radical-Controlled" Oxidative Polymerization of 4-Phenoxyphenol by a Tyrosinase Model Complex Catalyst to Poly(1,4-Phenylene Oxide). *Macromolecules* **2000**, *33*, 1986−1995.

(7) (a) Hay, A. S.; Blanchard, H. S.; Endres, G. F.; Eustance, J. W. Polymerization by Oxidative Coupling. *J. Am. Chem. Soc.* **1959**, *81*, 6335−6336. (b) Endres, G. F.; Hay, A. S.; Eustance, J. W. Polymerization by Oxidative Coupling. V. Catalytic Specificity in the Copper-Amine-Catalyzed Oxidation of 2,6-Dimethylphenol. *J. Org. Chem.* **1963**, *28*, 1300−1305.

(8) (a) Lee, Y. E.; Cao, T.; Torruellas, C.; Kozlowski, M. C. Selective Oxidative Homo- and Cross-Coupling of Phenols with Aerobic Catalysts. *J. Am. Chem. Soc.* **2014**, *136*, 6782−5. (b) Nieves-Quinones, Y.; Paniak, T. J.; Lee, Y. E.; Kim, S. M.; Tcyrulnikov, S.; Kozlowski, M. C. Chromium-Salen Catalyzed Cross-Coupling of Phenols: Mechanism and Origin of the Selectivity. *J. Am. Chem. Soc.* **2019**, *141*, 10016. (c) Reiss, H.; Shalit, H.; Vershinin, V.; More, N. Y.; Forckosh, H.; Pappo, D. Cobalt(II)[Salen]-Catalyzed Selective Aerobic Oxidative Cross-Coupling between Electron-Rich Phenols and 2-Naphthols. *J. Org. Chem.* **2019**, *84*, 7950.

(9) (a) Altwicker, E. R. The Chemistry of Stable Phenoxy Radicals. *Chem. Rev.* **1967**, *67*, 475−531. (b) Fitzpatrick, J. D.; Steelink, C.; Hansen, R. E. Phenoxy Radical Intermediates. II. The Oxidative Detoxification of Phenols in Incense Cedar Heartwood. *J. Org. Chem.* **1967**, *32*, 625−628. (c) Becconsall, J.; Clough, S.; Scott, G. Electron Magnetic Resonance of Phenoxy Radicals. *Trans. Faraday Soc.* **1960**, *56*, 459−472.

(10) Müller, E.; Schick, A.; Scheffler, K. Oxygen Radicals—XI. 4-Phenyl-2, 6-Di (*tert*-Butyl) Phenoxyl. *Chem. Ber.* **1959**, *92*, 474−482.

(11) (a) Manner, V. W.; Markle, T. F.; Freudenthal, J. H.; Roth, J. P.; Mayer, J. M. The First Crystal Structure of a Monomeric Phenoxyl Radical: 2,4,6-Tri-*tert*-Butylphenoxyl Radical. *Chem. Commun.* **2008**, 256−8. (b) Porter, T. R.; Kaminsky, W.; Mayer, J. M. Preparation, Structural Characterization, and Thermochemistry of an Isolable 4-Arylphenoxyl Radical. *J. Org. Chem.* **2014**, *79*, 9451−9454.

(12) Brigati, G.; Lucarini, M.; Mugnaini, V.; Pedulli, G. F. Determination of the Substituent Effect on the O−H Bond Dissociation Enthalpies of Phenolic Antioxidants by the Epr Radical Equilibration Technique. *J. Org. Chem.* **2002**, *67*, 4828−4832.

(13) Wang, Y.; Wang, G.; Yao, J.; Li, H. Restricting Effect of Solvent Aggregates on Distribution and Mobility of $CuCl_2$ in Homogenous Catalysis. *ACS Catal.* **2019**, *9*, 6588−6595.

(14) (a) Ritchie, C. D.; Sager, W. F. An Examination of Structure-Reactivity Relationships. *Prog. Phys. Org. Chem.* **2007**, *2*, 323−456. (b) Tribble, M. T.; Traynham, J. G. Nuclear Magnetic Resonance Studies of *ortho*-Substituted Phenols in Dimethyl Sulfoxide Solutions. Electronic Effects of Ortho Substituents. *J. Am. Chem. Soc.* **1969**, *91*, 379−388.

(15) Itoh, S.; Kumei, H.; Taki, M.; Nagatomo, S.; Kitagawa, T.; Fukuzumi, S. Oxygenation of Phenols to Catechols by a (μ-η^2:η^2-Peroxo)Dicopper(II) Complex: Mechanistic Insight into the Phenolase Activity of Tyrosinase. *J. Am. Chem. Soc.* **2001**, *123*, 6708−6709.

(16) Stoll, S.; Schweiger, A. Easyspin, a Comprehensive Software Package for Spectral Simulation and Analysis in Epr. *J. Magn. Reson.* **2006**, *178*, 42−55.

(17) Amorati, R.; Pedulli, G. F.; Guerra, M. Hydrogen Hyperfine Splitting Constants for Phenoxyl Radicals by DFT Methods: Regression Analysis Unravels Hydrogen Bonding Effects. *Org. Biomol. Chem.* **2010**, *8*, 3136−3141.

(18) McConnell, H. M. Indirect Hyperfine Interactions in the Paramagnetic Resonance Spectra of Aromatic Free Radicals. *J. Chem. Phys.* **1956**, *24*, 764−766.

https://dx.doi.org/10.1021/acs.inorgchem.9b02422
Inorg. Chem. XXXX, XXX, XXX−XXX

(19) Berho, F.; Lesclaux, R. The Phenoxy Radical: UV Spectrum and Kinetics of Gas-Phase Reactions with Itself and with Oxygen. *Chem. Phys. Lett.* **1997**, *279*, 289−296.
(20) Ghosh, S.; Cirera, J.; Vance, M. A.; Ono, T.; Fujisawa, K.; Solomon, E. I. Spectroscopic and Eectronic Structure Studies of Phenolate Cu(II) Complexes: Phenolate Ring Orientation and Activation Related to Cofactor Biogenesis. *J. Am. Chem. Soc.* **2008**, *130*, 16262−16273.
(21) Zombeck, A.; Drago, R. S.; Corden, B. B.; Gaul, J. H. Activation of Molecular Oxygen. Kinetic Studies of the Oxidation of Hindered Phenols with Cobalt-Dioxygen Complexes. *J. Am. Chem. Soc.* **1981**, *103*, 7580−7585.
(22) Company, A.; Yao, S.; Ray, K.; Driess, M. Dioxygenase-Like Reactivity of an Isolable Superoxo−Nickel(II) Complex. *Chem. - Eur. J.* **2010**, *16*, 9669−9675.
(23) (a) Houk, K. N.; Sims, J.; Duke, R. E.; Strozier, R. W.; George, J. K. Frontier Molecular Orbitals of 1,3 Dipoles and Dipolarophiles. *J. Am. Chem. Soc.* **1973**, *95*, 7287−7301. (b) Houk, K. N.; Sims, J.; Watts, C. R.; Luskus, L. J. Origin of Reactivity, Regioselectivity, and Periselectivity in 1,3-Dipolar Cycloadditions. *J. Am. Chem. Soc.* **1973**, *95*, 7301−7315. (c) Rozeboom, M. D.; Tegmo-Larsson, I. M.; Houk, K. N. Frontier Molecular Orbital Theory of Substitutent Effects on Regioselectivities of Nucleophilic Additions and Cycloadditions to Benzoquinones and Naphthoquinones. *J. Org. Chem.* **1981**, *46*, 2338−2345. (d) Mirzaei, S.; Khosravi, H. Predicting the Regioselectivity of Nucleophilic Addition to Arynes Using Frontier Molecular Orbital Contribution Analysis. *Tetrahedron Lett.* **2017**, *58*, 3362−3365.
(24) Kitajima, N.; Fujisawa, K.; Fujimoto, C.; Morooka, Y.; Hashimoto, S.; Kitagawa, T.; Toriumi, K.; Tatsumi, K.; Nakamura, A. A New Model for Dioxygen Binding in Hemocyanin. Synthesis, Characterization, and Molecular Structure of The μ-η^2:η^2 Peroxo Dinuclear Copper (II) Complexes,[Cu (HB (3, 5-R_2pz) $_3$)] $_2$ (O_2)(R= Isopropyl and Ph). *J. Am. Chem. Soc.* **1992**, *114*, 1277−1291.

https://dx.doi.org/10.1021/acs.inorgchem.9b02422
Inorg. Chem. XXXX, XXX, XXX−XXX